

## Characterization of the Reconstituted $\gamma$ -Secretase Complex from Sf9 Cells Co-Expressing Presenilin 1, Nicastrin, aph-1a, and pen-2

Lili Zhang,<sup>\*,‡</sup> Julie Lee,<sup>‡</sup> Lixin Song,<sup>‡</sup> Xiaoyan Sun,<sup>§</sup> Jie Shen,<sup>§</sup> Giuseppe Terracina,<sup>‡</sup> and Eric M. Parker<sup>‡</sup>

*Department of Neurobiology, Schering-Plough Research Institute, Kenilworth, New Jersey 07033, and Center for Neurologic Diseases, Brigham and Women's Hospital, Boston, Massachusetts 02115*

*Received August 26, 2004; Revised Manuscript Received November 24, 2004*

**ABSTRACT:**  $\gamma$ -Secretase catalyzes the proteolytic processing of a number of integral membrane proteins, including amyloid precursor protein (APP) and Notch. The native  $\gamma$ -secretase is a heterogeneous population of large membrane protein complexes containing presenilin 1 (PS1) or presenilin 2 (PS2), aph-1a or aph-1b, nicastrin, and pen-2. Here we report the reconstitution of a  $\gamma$ -secretase complex in Sf9 cells by co-infection with baculoviruses carrying the PS1, nicastrin, pen-2, and aph-1a genes. The reconstituted enzyme processes C99 and the Notch-like substrate N160 and displays the characteristic features of  $\gamma$ -secretase in terms of sensitivity to a  $\gamma$ -secretase inhibitor, upregulation of A $\beta$ 42 production by a familial Alzheimer's disease (FAD) mutation in the APP gene, and downregulation of Notch processing by PS1 FAD mutations. However, the ratio of A $\beta$ 42:A $\beta$ 40 production by the reconstituted  $\gamma$ -secretase is significantly higher than that of the native enzyme from 293 cells. Unlike in mammalian cells where PS1 FAD mutations cause an increase in A $\beta$ 42 production, PS1 FAD missense mutations in the reconstitution system alter the cleavage sites in the C99 substrate without changing the A $\beta$ 42:A $\beta$ 40 ratio. In addition, PS1 $\Delta$ E9 is a loss-of-function mutation in both C99 and N160 processing. Reconstitution of  $\gamma$ -secretase provides a homogeneous system for studying the individual  $\gamma$ -secretase complexes and their roles in A $\beta$  production, Notch processing and AD pathogenesis. These studies may provide important insight into the development of a new generation of selective  $\gamma$ -secretase inhibitors with an improved side effect profile.

$\gamma$ -Secretase catalyzes the intramembrane cleavage of the amyloid precursor protein (APP)<sup>1</sup> to generate two major species of  $\beta$ -amyloid peptides (A $\beta$ ) (reviewed in ref 1). A $\beta$ 40 comprises 90–95% of all A $\beta$  produced by  $\gamma$ -secretase, while A $\beta$ 42, although comprising only 5–10% of A $\beta$  production, is the major constituent of amyloid plaques and is thought to play a more critical role in the pathogenesis of Alzheimer's disease (AD). In addition to APP,  $\gamma$ -secretase also cleaves numerous other membrane proteins such as Notch, ErbB4, CD44, and the Notch ligands Delta1 and Jagged2 (2–5), all of which exhibit little sequence homology around the cleavage site. The mechanism by which  $\gamma$ -secretase specifically cleaves multiple substrates with distinct structures is not clear.  $\gamma$ -Secretase is an attractive target for AD therapy, but the presence of Notch and other substrates can potentially be the major cause of undesirable biological effects (6).

$\gamma$ -Secretase is believed to be a large complex that contains at least four membrane proteins: PS1 or PS2, nicastrin (NCT), pen-2, and aph-1a or aph-1b (reviewed in ref 7). Both PS1 and PS2 exist as heterodimers of N-terminal and C-terminal fragments (NTF and CTF, respectively) (8). Although genetic studies have shown that all four proteins

are essential for  $\gamma$ -secretase activity (9–11), the specific function of each protein in the complex is less clear. The multi-transmembrane domain proteins PS1 and PS2 are the first components identified in this complex and are also considered to be likely candidates for the catalytic subunit of  $\gamma$ -secretase (12). More than 80 clinical mutations are found in the PS1 gene and six in the PS2 gene, all of which selectively promote cellular A $\beta$ 42 production (1). Most of the  $\gamma$ -secretase inhibitors studied to date are nonselective for PS1 and PS2  $\gamma$ -secretases (13–15). Studies on the PS1 and PS2 deficient cells demonstrate that PS1 plays a major role in cellular A $\beta$  production (9). PS2 deletion, while having little impact on A $\beta$  production (16), can accelerate the pathological changes caused by PS1 deficiency (17, 18). These data suggest that  $\gamma$ -secretase inhibitors with selectivity of PS1 over PS2 may significantly improve the side effect profile of the current generation of compounds. Developing a  $\gamma$ -secretase inhibitor with selectivity for a specific subtype of  $\gamma$ -secretase complex, however, has been limited by the heterogeneous nature of the native  $\gamma$ -secretase.

Reconstitution of a  $\gamma$ -secretase complex has recently been achieved by co-expressing the four components in yeast, an organism lacking endogenous  $\gamma$ -secretase activity (19). This finding provides strong evidence that PS, NCT, aph-1, and pen-2 are indeed sufficient for reconstitution of  $\gamma$ -secretase activity. However, the yeast expression system is not readily amenable to biochemical studies. We report here the reconstitution of  $\gamma$ -secretase activity in Sf9 insect cells by co-infecting cells with baculoviruses expressing PS1, NCT,

\* To whom correspondence should be addressed. Telephone: (908) 740-6559. Fax: (908) 740-2383. E-mail: lili.zhang@spcorp.com.

<sup>‡</sup> Schering-Plough Research Institute.

<sup>§</sup> Brigham and Women's Hospital.

<sup>1</sup> Abbreviations: A $\beta$ ,  $\beta$ -amyloid peptide; AD, Alzheimer's disease; APP, amyloid precursor protein; AICD, APP intracellular domain; FAD, familial Alzheimer's disease; NCT, nicastrin; NICD, Notch intracellular domain; PS, presenilin.

aph-1a, and pen-2. A detailed biochemical analysis of this reconstituted activity revealed the characteristics of  $\gamma$ -secretase as well as the features that are distinct from those of the native enzyme. The reconstitution in Sf9 cells provides an important tool for exploring the assembly of the  $\gamma$ -secretase complex and a homogeneous system for studying the biochemical properties of each individual  $\gamma$ -secretase activity.

## EXPERIMENTAL PROCEDURES

**Expression Constructs.** Human PS1 and NCT cDNAs were obtained from P. St. George-Hyslop (University of Toronto, Toronto, ON). Human pen-2 (11) and aph-1a (20) cDNAs were cloned from a human brain cDNA library (Clontech). A myc tag and six-His tag were introduced at the C-termini of NCT and aph-1 and at the N-terminus of pen-2. Baculoviruses carrying PS1, NCT, pen-2, and aph-1a cDNAs were generated using the BAC-to-BAC system (Invitrogen) according to the manufacturer's instructions.

**Cell Culture.** Human embryonic kidney 293 cells were purchased from American Type Culture Collection and were grown in Dulbecco's modified Eagle's medium (DMEM) supplemented with 10% fetal bovine serum, 100 units/mL penicillin, and 100  $\mu$ g/mL streptomycin. Sf9 insect cells were purchased from Invitrogen and were grown in Sf900 II serum-free medium (Invitrogen) supplemented with 3% fetal bovine serum. To express a designated protein, Sf9 cells ( $1 \times 10^6$  cells/mL) were infected with the appropriate baculovirus and harvested 3 days after infection. For mock infection, a baculovirus carrying human  $11\beta$ -hydroxysteroid dehydrogenase was used.

**Membrane Preparations.** A quick, crude membrane preparation procedure was used to study multiple reconstitution conditions in Sf9 cells. Cells from a 100 mL culture were harvested and washed once in cold phosphate-buffered saline. The cell pellets were resuspended in a buffer containing 20 mM Tris-HCl (pH 7), 50 mM KCl, 50 mM sucrose, 2 mM EDTA, 2 mM EGTA, and Complete protease inhibitor tablets (Roche Biochemicals), and homogenized with a 20 s pulse using a PowerGen 125 homogenizer at full power. The homogenate was centrifuged at 15000g for 30 min. The membrane pellets were solubilized in a buffer containing Tris-HCl (pH 7.0), 150 mM NaCl, 2 mM EDTA, 2 mM EGTA, and 1% CHAPSO, and insoluble components were removed by centrifugation at 100000g for 45 min.

PS1 M146V knock-in mice have been described previously (21). Membranes were prepared from individual cortices and solubilized in 1% CHAPSO. Membrane preparation from 293 cells was as described previously (22).

**Measurement of  $\gamma$ -Secretase Activity.** To measure  $\gamma$ -secretase activity, a 50  $\mu$ L reaction mixture was assembled by combining the C99 substrate (22) and 10–20  $\mu$ g of the solubilized membrane protein in a buffer containing 50 mM acetate (pH 6.0), 100 mM NaCl, 2 mM EDTA, and 0.2% CHAPSO. The reaction was carried out at 37 °C for 2 h. A $\beta$ 40 and A $\beta$ 42 were assessed using a sandwich immunoassay as described previously (23), while the C-terminal cleavage product (AICD) was detected by Western blotting using antibody 369. The  $\gamma$ -secretase inhibitor used in some experiments, L-684,458 (24), was purchased from Calbiochem.

**Measurement of Notch Processing Activity.** Human Notch1 (GenBank entry AF308602) with a truncated extracellular

domain (N $\Delta$ E) was cloned from human fetal cDNA (Clontech). This fragment was further truncated by deleting amino acids 1772–2153, which preserved the  $\gamma$ -secretase cleavage site and resulted in a Notch-like substrate designated N160. N160 with C-terminal myc and six-His tags was expressed in Sf9 cells and purified by Ni-NTA chromatography as described for C99 purification (22). To assess N160 processing by  $\gamma$ -secretase, 2  $\mu$ M N160 was combined with 5–15  $\mu$ g of the solubilized membrane protein in the same reaction buffer that was used for  $\gamma$ -secretase activity (see above). The reaction was carried out at 37 °C for 4 h. The C-terminal fragment generated by  $\gamma$ -secretase cleavage, NICD160, was detected by Western blotting using a cleavage site specific antibody (Cell Signaling).

**Immunoprecipitation.** To study proteins associated with PS1, 50  $\mu$ L of CHAPSO-solubilized membranes from Sf9 cells (3 mg of protein/mL) was incubated overnight with 1  $\mu$ L of anti-PS1 NTF antibody (Cell Signaling) at 4 °C. Protein A/G beads (Calbiochem) were added, and the mixture was rocked at 4 °C for an additional 2 h. The beads were then spun down and washed three times in a buffer containing 20 mM Tris-HCl (pH 7.4), 150 mM NaCl, 2 mM EDTA, 2 mM EGTA, and 0.5% CHAPSO. After removal of the washing buffer, proteins were eluted from the beads and separated on a 4 to 12% NuPAGE gel (Invitrogen).

**General Methods.** Anti-PS1 NTF antibody and anti-myc antibody were purchased from Cell Signaling. Protein concentrations were determined using the Protein Assay Dye (Bio-Rad) according to the manufacturer's instructions.

## RESULTS

**Reconstitution of the  $\gamma$ -Secretase Complex in Sf9 Cells.** Although insect cells contain a PS gene (25), the endogenous PS protein in Sf9 cells did not cross-react with an anti-human PS1 antibody (Figure 1A). Nevertheless, solubilized Sf9 cell membranes do have endogenous  $\gamma$ -secretase activity, but this activity was abolished upon infection with baculovirus (Figure 1B). This loss of activity is likely due to the disruption of Sf9 cell protein synthesis by virus infection, thus affecting the protein turnover in the endogenous  $\gamma$ -secretase complex. Baculovirus-mediated protein expression in Sf9 cells thus provides an opportunity to study the reconstitution of  $\gamma$ -secretase and the role of each component in catalytic activity without the interference of background activity.

When PS1, NCT, aph-1, and pen-2 were expressed in Sf9 cells by co-infection of the four baculoviruses, a significant amount of full-length PS1 was processed to NTF (Figure 1A). The processing of PS1 was dramatically inhibited when any one of the components was missing, suggesting that NCT, aph-1, and pen-2 are all required for the efficient proteolytic maturation of PS1. Mutations of two conserved aspartyl residues in the PS1 gene that are known to be critical for  $\gamma$ -secretase activity, D257A and D385A, abolished PS1 processing (Figure 1A). Accompanying the processing of PS1, robust  $\gamma$ -secretase activity was observed in solubilized membranes from Sf9 cells co-infected with baculoviruses expressing PS1, pen-2, aph-1, and NCT. This activity was 3–5-fold higher than the endogenous activity in uninfected Sf9 cells (cf. panels B and C of Figure 1) and was undetectable when any one of the proteins was missing

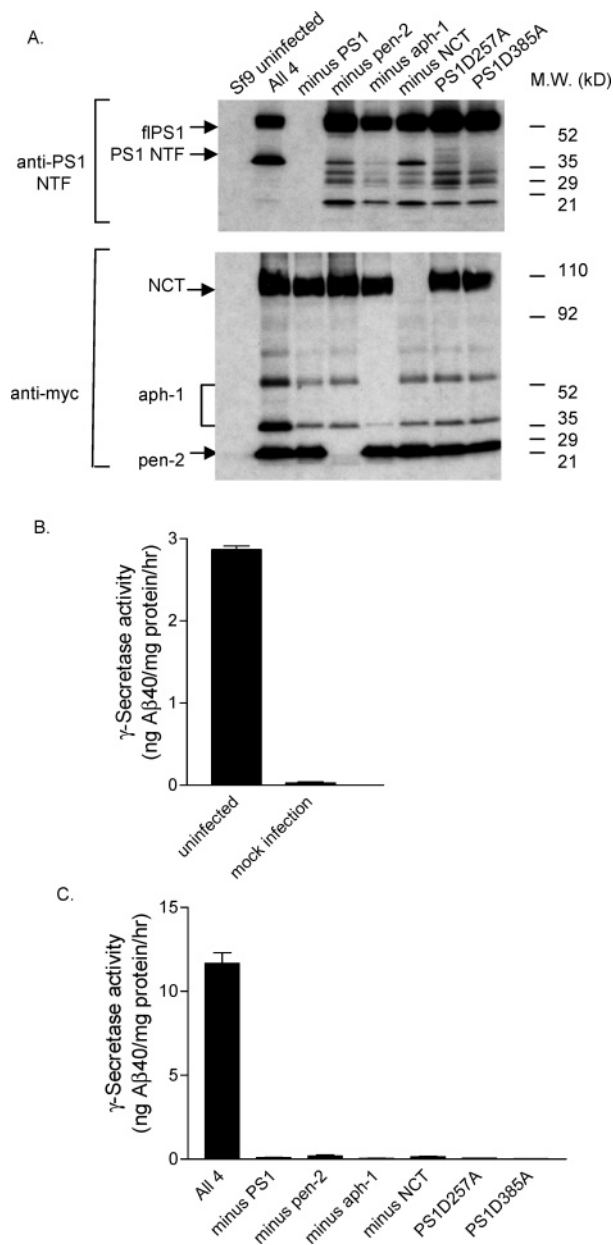


**FIGURE 1:** Reconstitution of  $\gamma$ -secretase activity in Sf9 cells. Solubilized membrane fractions were prepared from Sf9 cells infected with specified baculoviruses. (A) Western blots of solubilized membranes from Sf9 cells probed with the anti-PS1 NTF antibody for PS1 expression or the anti-myc antibody for NCT, pen-2, and aph-1 expression. Several bands with molecular weights similar to or lower than that of PS1 NTF reacted with the anti-PS1 NTF antibody, but were likely nonspecific degradation products. Two bands were associated with aph-1 expression, and the top band was likely a dimmer as judged by molecular weight. (B)  $\gamma$ -Secretase activity in membranes prepared from wild-type and baculovirus-infected Sf9 cells. The baculovirus used in the mock infection carries the human 11 $\beta$ -hydroxysteroid dehydrogenase gene. Several other baculoviruses expressing various unrelated cDNAs were also tested, and similar abolition of  $\gamma$ -secretase activity was obtained (L. Song and L. Zhang, unpublished data). (C)  $\gamma$ -Secretase activity in Sf9 cell membranes expressing various combinations of the components of the  $\gamma$ -secretase complex.

(Figure 1C), consistent with the notion that all four components are essential for  $\gamma$ -secretase function. PS1-D257A and PS1-D385A failed to reconstitute  $\gamma$ -secretase activity when co-expressed with the other three proteins (Figure 1C), confirming that they are indeed loss-of-function mutations (12).

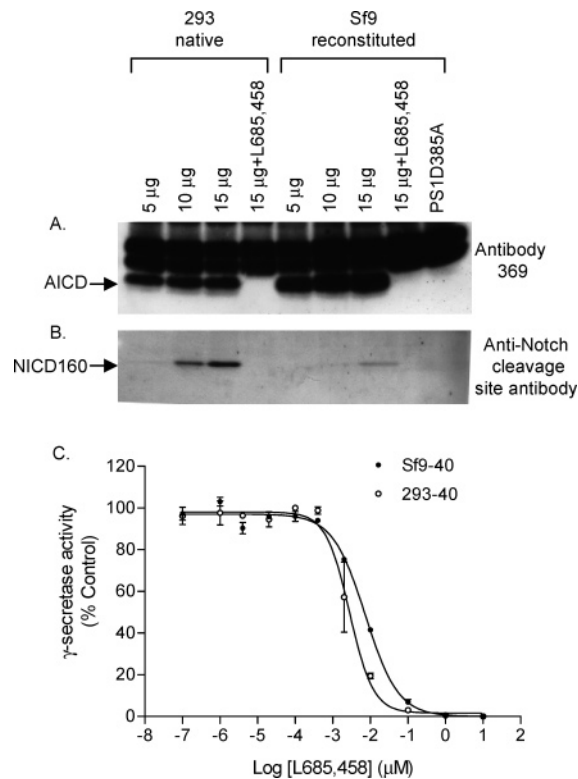


**FIGURE 2:** AICD and NICD160 production by reconstituted  $\gamma$ -secretase. N160 or C99 substrate was incubated with solubilized membranes (5–15  $\mu$ g/reaction) from 293 cells or from Sf9 cells expressing all four components of the  $\gamma$ -secretase complex. The reaction mixtures were separated on a 4 to 12% NuPAGE gel with MES buffer (Invitrogen). (A) Generation of AICD from the C99 substrate. The APP intracellular domain (AICD), released after cleavage of C99 at all  $\gamma$ -secretase sites including 40, 42, and  $\epsilon$ , was detected by antibody 369. (B) Generation of NICD160 from N160 substrate. NICD160 was detected by a cleavage site specific antibody. (C) Effect of the  $\gamma$ -secretase inhibitor L-685,458 on the reconstituted and native enzyme.  $\gamma$ -Secretase activity was measured using 2  $\mu$ M C99 substrate in the presence of different concentrations of L-685,458.

The reconstituted  $\gamma$ -secretase complex displayed activity comparable to that of the native enzyme in human embryonic kidney 293 cell membranes in terms of its ability to cleave the C99 substrate to generate the AICD products (Figure 2A). In addition, the reconstituted  $\gamma$ -secretase was also capable of processing a truncated Notch substrate (N160) to generate NICD160 as detected by a Notch cleavage site specific antibody (Figure 2B). Both AICD production and NICD160 production were abolished by a well-characterized  $\gamma$ -secretase inhibitor, L-685,458 (24), and by the D385A mutation (Figure 2A,B). Furthermore, L-685,458 inhibits the reconstituted enzyme activity with an  $IC_{50}$  of 7 nM, which was similar to the action of this compound on the native enzyme [ $IC_{50}$  = 3 nM (Figure 2C)].

Like the enzyme in 293 cell membranes (Figure 3A), the reconstituted  $\gamma$ -secretase from Sf9 cells generated both A $\beta$ 40 and A $\beta$ 42 (Figure 3B). The  $K_m$  values of the reconstituted enzyme for A $\beta$ 40 and A $\beta$ 42 activity were  $1.2 \pm 0.6$  and  $1.6 \pm 0.7$   $\mu$ M, respectively, which were similar to the  $K_m$  values of the native  $\gamma$ -secretase activity ( $0.5 \pm 0.2$  and  $1.2 \pm 0.7$   $\mu$ M for A $\beta$ 40 and A $\beta$ 42 activity, respectively). The A $\beta$ 42:A $\beta$ 40 ratio of activity in solubilized 293 cell membranes was similar to the endogenous  $\gamma$ -secretase activity in solubilized Sf9 cell membranes (Figure 3C), and was consistent with

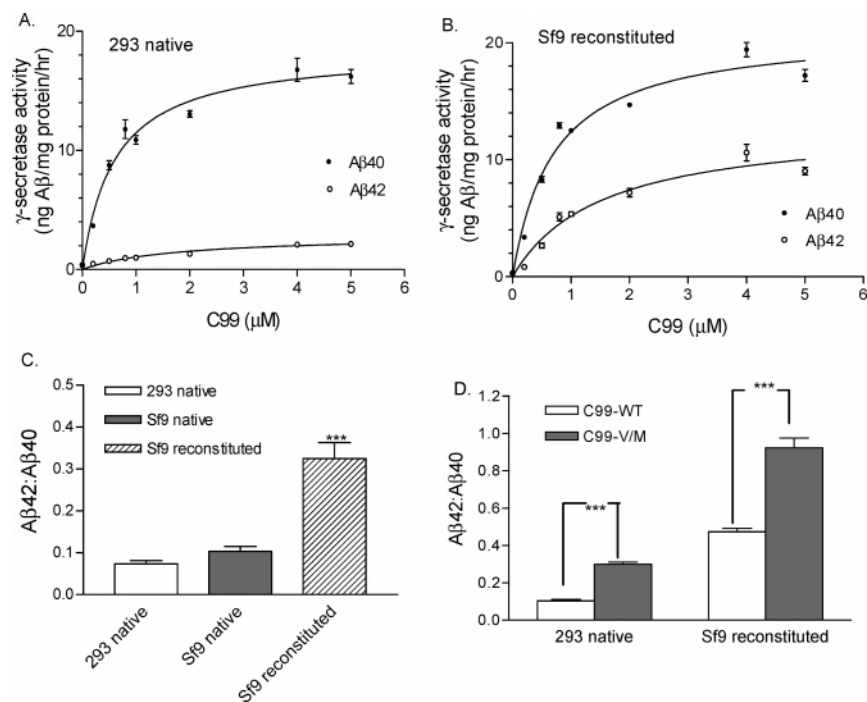


FIGURE 3: A $\beta$ 40 and A $\beta$ 42 production by the reconstituted  $\gamma$ -secretase activity.  $\gamma$ -Secretase activity in membranes from Sf9 cells co-expressing PS1, NCT, pen-2, and aph-1 was determined as described in Experimental Procedures. (A) A $\beta$ 40 and A $\beta$ 42  $\gamma$ -secretase activity from 293 cells. (B) A $\beta$ 40 and A $\beta$ 42 activity from reconstituted  $\gamma$ -secretase. (C) Comparison of the A $\beta$ 42:A $\beta$ 40 ratio of native  $\gamma$ -secretase from 293 cells, endogenous  $\gamma$ -secretase activity in Sf9 cells and the reconstituted  $\gamma$ -secretase activity in Sf9 cells. A $\beta$ 42 production and A $\beta$ 40 production were assessed using C99 substrate concentrations of 1–5  $\mu$ M. (D) Effect of the APP V715M mutation on the A $\beta$ 42:A $\beta$ 40 ratio. The A $\beta$ 42:A $\beta$ 40 ratios were measured using 1–5  $\mu$ M wild-type and V/M mutant substrates. The error bars represent the standard errors from three independent experiments. Data were analyzed with the *t* test using GraphPad Prism 3.0. Three asterisks indicate *P* < 0.001.

the A $\beta$ 42:A $\beta$ 40 ratio detected in conditioned media from various cell lines and brain lysates (26, 27). The reconstituted  $\gamma$ -secretase activity, however, displayed a significantly higher A $\beta$ 42:A $\beta$ 40 ratio (Figure 3C). To further explore A $\beta$ 42 activity by the reconstituted enzyme, we utilized a C99 substrate carrying the APP V715M mutation in the APP770 gene. This mutation is located two amino acids after the A $\beta$ 42 cleavage site and is linked to enhanced cellular A $\beta$ 42 production and early onset AD (28). The APP V715M mutation in C99 did not change the substrate interaction with  $\gamma$ -secretase, as the  $K_m$  values for A $\beta$ 40 and A $\beta$ 42 were similar to that of the wild-type substrate (L. Zhang, unpublished data), but the A $\beta$ 42:A $\beta$ 40 activity ratio was significantly higher than that of the wild-type substrate (Figure 3D). The impact of the APP V715M mutation on A $\beta$ 42 production was similar for the native enzyme from 293 cells and the reconstituted enzyme from Sf9 cells, suggesting that the preference of the active sites for A $\beta$ 42 cleavage are similarly affected by the V715M mutation. Overall, these findings are consistent with the reported reconstitution of  $\gamma$ -secretase activity in yeast (19) and demonstrate that the reconstituted  $\gamma$ -secretase displays several characteristics of the native enzyme, but also displays at least one distinct property, namely, the enhanced A $\beta$ 42 production.

**Effect of PS1 FAD Mutations on Reconstituted  $\gamma$ -Secretase Activity.** We utilized the reconstituted system to examine the effect of PS1 FAD mutations on  $\gamma$ -secretase complex assembly, PS1 endoproteolysis, and the enzymatic activity. NCT, pen-2, and aph-1 co-immunoprecipitated with all PS1 mutants, including Y115H, M146L, L392V,  $\Delta$ E9, and D385A (Figure 4A), suggesting that these mutations did not have an impact on the formation of the  $\gamma$ -secretase complex

in Sf9 cells. The three FAD missense mutations, Y115H, M146L, and L392V, were processed properly, whereas the D385A and  $\Delta$ E9 mutations remained unprocessed in the reconstituted complex (Figure 4B). These results are consistent with reported observations of the native enzyme in mammalian cells.

In the reconstituted  $\gamma$ -secretase complex, total  $\gamma$ -secretase activity as measured by AICD production was comparable for the PS1 Y115H, M146L, and L392V mutations (Figure 5A). In contrast, NICD160 production and A $\beta$  production were impaired by these mutations, with Y115H having the greatest impact and M146L the least (Figures 5B and 6A). The PS1  $\Delta$ E9 mutant was inactive in both AICD and NICD160 production (Figure 5A,B). The M146L and L392V mutations reduced the  $V_{max}$  of A $\beta$  production without significantly changing the  $K_m$  for either A $\beta$ 40 or A $\beta$ 42 activity (Figure 6B,C). The level of A $\beta$  production was too low for Y115H for reliable quantification (data not shown). No significant effect on the A $\beta$ 42:A $\beta$ 40 ratio was observed with the M146L and L392V mutations (Figure 6D). Interestingly,  $\gamma$ -secretase activity in soluble membranes from brains of PS1M146V knock-in mice (21) displayed a modest reduction in A $\beta$ 40 activity, an increase in A $\beta$ 42 activity, and consequently a significant increase in the A $\beta$ 42:A $\beta$ 40 ratio (Figure 7A–C). These results thus demonstrate that the FAD mutations behave differently in the reconstituted  $\gamma$ -secretase complex compared to the native enzyme in mouse brain membranes in terms of A $\beta$ 42 production.

## DISCUSSION

Our study demonstrates the reconstitution of  $\gamma$ -secretase activity by the simultaneous infection of Sf9 insect cells with

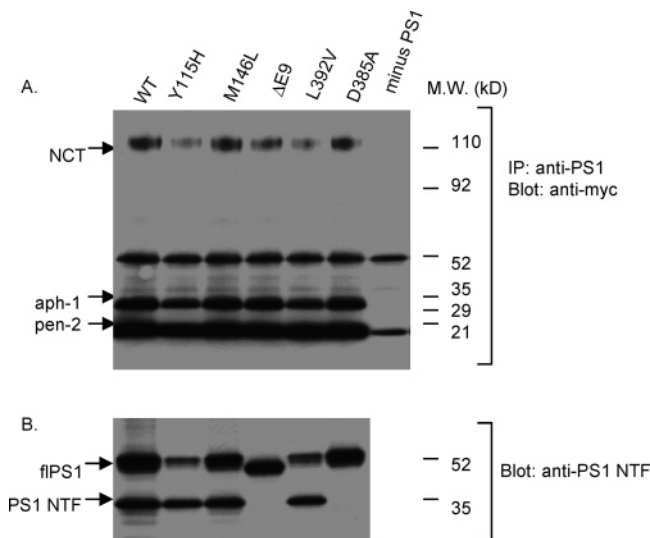


FIGURE 4: Effect of PS1 FAD mutations on the assembly of the  $\gamma$ -secretase complex and the processing of PS1. Membranes were prepared from Sf9 cells co-infected with baculoviruses expressing pen-2, aph-1, NCT, and either wild-type PS1 or PS1 mutant Y115H, M146L,  $\Delta$ E9, L392V, or D385A. (A) Effect of FAD mutations on the assembly of the  $\gamma$ -secretase complex.  $\gamma$ -Secretase complexes were immunoprecipitated from CHAPSO-solubilized membrane preparations with anti-PS1 NTF antibody. The immunoprecipitated proteins were separated on a 4 to 12% NuPAGE gel and probed with anti-myc antibody. Bands corresponding to NCT, aph-1, and pen-2 are shown. The background was defined using the membranes from Sf9 cells co-infected with NCT, aph-1, and pen-2 but without PS1. (B) Effect of PS1 FAD mutations on PS1 processing. Western blots of solubilized membranes were probed with anti-PS1 NTF antibody.

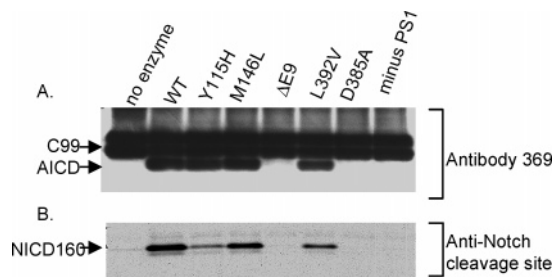


FIGURE 5: Effects of PS1 FAD mutations on C99 and N160 processing. Membranes were prepared as described in the legend of Figure 4.  $\gamma$ -Secretase activity was measured using the solubilized membranes as described in Experimental Procedures and in the legend of Figure 2. (A) C99 processing to AICD as detected by Western blotting with antibody 369. (B) N160 processing to NICD160 detected by Western blotting with an anti-Notch cleavage site specific antibody.

four baculoviruses carrying the PS1, NCT, pen-2, and aph-1 genes. Many of the characteristics of the reconstituted  $\gamma$ -secretase activity from Sf9 cells are similar to those described for the native enzyme. The reconstituted  $\gamma$ -secretase is capable of generating  $A\beta$ 40 and  $A\beta$ 42 with appropriate kinetics (Figure 3A,B), and generates AICD (Figure 2A) and the Notch cleavage product NICD160 (Figure 2B). This activity can also be blocked by a prototype  $\gamma$ -secretase inhibitor (Figure 2C) and produce more  $A\beta$ 42 when the APP V715M mutation is introduced into the C99 substrate (Figure 3D). In the reconstituted  $\gamma$ -secretase complex, the PS1 FAD missense mutations slow  $A\beta$ 40,  $A\beta$ 42, and NICD160 production to various degrees (Figures 5B and 6A) without significantly changing the AICD production (Figure 5A).

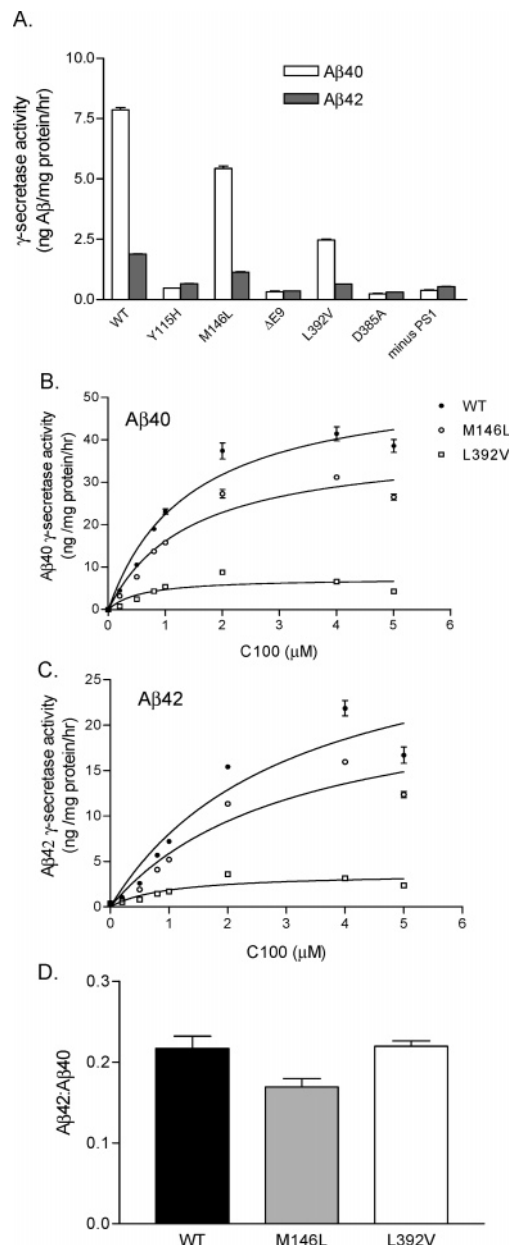


FIGURE 6: Effect of PS1 FAD mutations on the reconstituted  $A\beta$ 40 and  $A\beta$ 42  $\gamma$ -secretase activity. Membranes were prepared from Sf9 cells expressing various PS1 mutants, NCT, pen-2, and aph-1. (A)  $A\beta$ 40 and  $A\beta$ 42  $\gamma$ -secretase activity measured at 2  $\mu$ M C99. (B)  $A\beta$ 40  $\gamma$ -secretase activity at various C99 concentrations in the solubilized membranes from wild-type PS1-, PS1-M146L-, and PS1-L392V-infected Sf9 cells. (C)  $A\beta$ 42  $\gamma$ -secretase activity in membranes from wild-type PS1-, PS1-M146L-, and PS1-L392V-infected Sf9 cells. (D)  $A\beta$ 42: $A\beta$ 40 ratio determined in membranes from wild-type PS1-, PS1-M146L-, and PS1-L392V-infected Sf9 cells. The data are the mean of three independent experiments that measured the  $A\beta$ 42: $A\beta$ 40 ratio at 1–4  $\mu$ M C99 substrate.

This finding suggests that these mutations lead to a shift of cleavage site specificity, rather than a loss of catalytic function of the  $\gamma$ -secretase complex, which is consistent with the observation in mammalian cells that the enhanced cleavage at the  $A\beta$ 42 site mediated by PS1 FAD mutations is at the expense of the cleavage at the  $\epsilon$  site (29, 30). The decrease in the level of NICD160 production is also consistent with the reduced efficiency of PS1 FAD mutations in rescuing sel-12 deficiency in *Caenorhabditis elegans* (31). Overall, the reconstituted enzyme reflects many of the

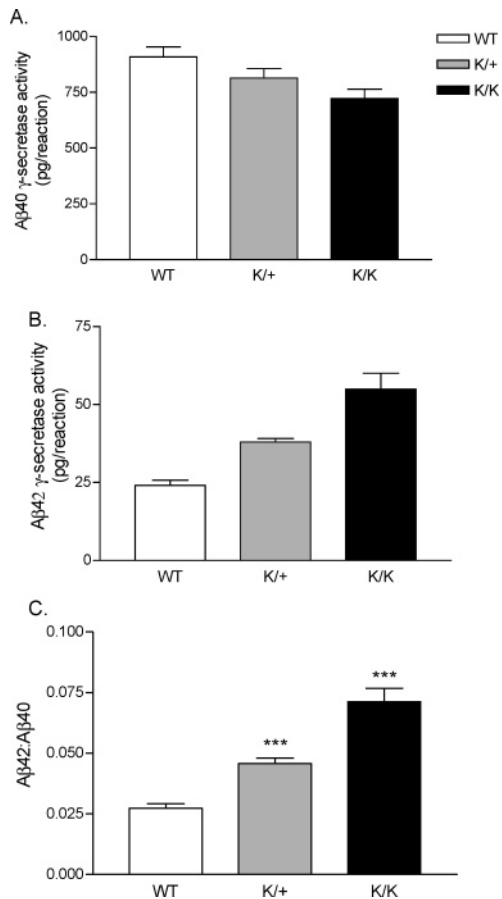


FIGURE 7:  $\gamma$ -Secretase activity from PS1-M146V knock-in mice brains. Membranes were prepared from individual brains of wild-type (WT), PS1-M146V knock-in heterozygote (K/+), and homozygote (K/K) mice.  $A\beta 40$  and  $A\beta 42$   $\gamma$ -secretase activities shown here were measured at 2  $\mu$ M C99, and the same trend was seen with the activities measured at 1 and 4  $\mu$ M C99 (data not shown). Brains of different genotypes had comparable levels of PS1 expression as detected by Western blot analysis (data not shown): (A)  $A\beta 40$   $\gamma$ -secretase activity, (B)  $A\beta 42$   $\gamma$ -secretase activity, and (C) comparison of  $A\beta 42:A\beta 40$  ratios in wild-type, heterozygote, and homozygote mice. The data shown are the mean  $\pm$  the standard errors calculated from three animals, each measured at three different substrate concentrations. Data were analyzed with the  $t$  test using GraphPad Prism 3.0. Three asterisks indicate  $P < 0.001$ .

fundamental properties of the native  $\gamma$ -secretase, and thus provides an important tool for studying the mechanism of its catalytic function.

Our study also reveals that the characteristics of  $\gamma$ -secretase are not fully recapitulated in the reconstitution system. The disparities are reflected largely in the regulation of  $A\beta 42$  production. In the reconstituted enzyme, the  $A\beta 42:A\beta 40$  ratio is significantly higher than that of the native enzyme in 293 cells (Figure 3). In addition, even though the three PS1 FAD missense mutations in the reconstituted  $\gamma$ -secretase complex alter the production of  $A\beta 40$  and  $A\beta 42$  by a mechanism similar to that in the native enzyme, they do not cause an increase in the  $A\beta 42:A\beta 40$  ratio of the reconstituted  $\gamma$ -secretase activity (Figure 6D) as they do in mammalian cells (22) and in mouse brains (Figure 7). Moreover, the PS1  $\Delta E9$  mutation is a complete loss-of-function mutation with respect to  $A\beta 40$ ,  $A\beta 42$ , AICD, and NICD160 production in the reconstituted  $\gamma$ -secretase (Figures 5 and 6). This is in contrast with the properties of the other PS1 missense mutations in the reconstitution system and the observation in mammalian

cells where overexpression of the PS1  $\Delta E9$  mutation leads to an elevated level of  $A\beta 42$  production without significantly affecting  $A\beta 40$  (26). The phenotype of the PS1  $\Delta E9$  mutant in reconstituted  $\gamma$ -secretase is also distinct from that seen in *C. elegans*, where it is similar to the other PS FAD mutations in acting as a partial loss-of-function mutation in terms of rescuing sel-12 deficiency (31).

Many factors may be responsible for the differences between the reconstituted  $\gamma$ -secretase and the native enzyme. NCT is a glycoprotein (10), and glycosylation in Sf9 cells differs from that in mammalian cells (32). While NCT is assembled into the active  $\gamma$ -secretase complex in the reconstitution system, the distinct glycosylation pattern of NCT in Sf9 cells may cause subtle change in its interaction with other components which may change the cleavage site specificity. The presence of N- and C-terminal epitope tags in the pen-2, aph-1, and NCT constructs could be another source of conformational change in the complex, although expression of these tagged constructs in mammalian cells has not been shown to alter  $A\beta 42$  production (10, 33–35; J. Lee and L. Zhang, unpublished data). In addition, despite the fact that none of the endogenous PS, NCT, pen-2, and aph-1 genes can be incorporated into the reconstituted functional  $\gamma$ -secretase complex (Figure 1) and that endogenous  $A\beta 42$   $\gamma$ -secretase activity in Sf9 cells is similar to that in 293 cells (Figure 3C), we still cannot completely exclude the possibility that some endogenous proteins in Sf9 cells are involved in the reconstitution process.

More importantly, the native  $\gamma$ -secretase activity reflects that of a heterogeneous population of  $\gamma$ -secretase complexes in mammalian cells. The presence of different PS genes (PS1 and PS2), aph-1 isoforms (aph-1a and aph-1b), and perhaps other unidentified factors can all contribute to the heterogeneity of the native enzyme. It is thus likely that the reconstituted  $\gamma$ -secretase complex described here reflects only one aspect of the native activity. The reconstitution in Sf9 cells provides a unique homogeneous system for further characterizing individual  $\gamma$ -secretase complexes and distinguishing their roles in  $A\beta$  production, Notch processing, and AD pathogenesis. A homogeneous system is also critical for developing subtype selective  $\gamma$ -secretase inhibitors with an improved side effect profile if the compound targets only one or two specific  $\gamma$ -secretase complexes involved in the disease process.

It is noteworthy that despite the overexpression of the four components, the specific activity of the reconstituted  $\gamma$ -secretase remains comparable to that of the native enzyme in 293 cells (Figure 3A,3B), and a significant amount of PS1 still remains unprocessed (Figure 1A). These data suggest that the limiting step for PS1 processing and assembly of the  $\gamma$ -secretase complex has not been resolved in the reconstitution system. It is not clear whether the four components are sufficient for this process or whether additional unidentified cellular proteins are required.

While we have successfully reconstituted many of the fundamental properties of  $\gamma$ -secretase, this study shows that the intricacies of the  $\gamma$ -secretase complex have not yet been completely elucidated. Future studies on the mechanism that limits the processing of PS1 may lead to a more efficient reconstitution system and facilitate the ultimate purification of the  $\gamma$ -secretase complex. Further unraveling of the mechanism that regulates the specific cleavage activity of

$\gamma$ -secretase will also be critical in understanding the broad spectrum of  $\gamma$ -secretase substrates and the pathogenic mechanism of PS FAD mutations. It may also provide important insight into the development of novel  $\gamma$ -secretase inhibitors that target more specifically APP processing and/or A $\beta$ 42 production.

While this paper was being prepared, reconstitution of  $\gamma$ -secretase activity was reported in budded baculovirus particles released from Sf9 cells co-infected with PS1, NCT, aph-1, and pen-2 (36). The reconstituted  $\gamma$ -secretase activities are comparable in both studies, although the reconstituted activity described here is from regular cellular membrane preparations, which do not have detectable endogenous  $\gamma$ -secretase-like activity as in the baculovirus particles.

## ACKNOWLEDGMENT

We thank Dr. Diane Levitan for critically reading the manuscript. We also thank Drs. Peter St. George-Hyslop and Gang Yu (University of Toronto) for the nicastrin cDNA construct and Huaxi Xu (Burnham Institute, La Jolla, CA) for antibody 369.

## REFERENCES

- Selkoe, D. (2001) Alzheimer's disease: Genes, proteins, and therapy, *Physiol. Rev.* 81, 741–766.
- Schroeter, E. H., Kisslinger, J. A., and Kopan, R. (1998) Notch-1 signalling requires ligand-induced proteolytic release of intracellular domain, *Nature* 393, 382–386.
- Ni, C.-Y., Murphy, M. P., Golde, T. E., and Carpenter, G. (2001)  $\gamma$ -Secretase cleavage and nuclear localization of ErbB-4 receptor tyrosine kinase, *Science* 294, 2179–2181.
- Lammich, S., Okochi, M., Takeda, M., Kaether, C., Capell, A., Zimmer, A. K., Edbauer, D., Walter, J., Steiner, H., and Haass, C. (2002) Presenilin-dependent intramembrane proteolysis of CD44 leads to the liberation of its intracellular domain and the secretion of an A $\beta$ -like peptide, *J. Biol. Chem.* 277, 44754–44759.
- Ikeuchi, T., and Sisodia, S. S. (2003) The Notch ligands, Delta1 and Jagged2, are substrates for presenilin-dependent " $\gamma$ -secretase" cleavage, *J. Biol. Chem.* 278, 7751–7754.
- Wong, G. T., Manfra, D., Poulet, F. M., Zhang, Q., Josien, H., Bara, T., Engstrom, L., Pinzon-Ortiz, M., Fine, J. S., Lee, H. J., Zhang, L., Higgins, G. A., and Parker, E. M. (2004) Chronic treatment with the  $\gamma$ -secretase inhibitor LY-411,575 inhibits  $\beta$ -amyloid peptide production and alters lymphopoiesis and intestinal cell differentiation, *J. Biol. Chem.* 279, 12876–12882.
- De Strooper, B. (2003) Aph-1, pen-2 and nicastrin with presenilin generate an active  $\gamma$ -secretase complex, *Neuron* 38, 9–12.
- Thinakaran, G., Borchelt, D. R., Lee, M. K., Slunt, H. H., Spitzer, L., Kim, G., Ratovitsky, T., Davenport, F., Nordstedt, C., Seeger, M., Hardy, J., Ai, L., Gandy, S. E., Jenkins, N. A., Copeland, N. G., Price, D. L., and Sisodia, S. S. (1996) Endoproteolysis of presenilin 1 and accumulation of processed derivatives in vivo, *Neuron* 17, 181–190.
- De Strooper, B., Saftig, P., Craessaerts, K., Vanderstichele, H., Guhde, G., Annaert, W., Von Figura, K., and Van Leuven, F. (1998) Deficiency of presenilin-1 inhibits the normal cleavage of amyloid precursor protein, *Nature* 391, 387–390.
- Yu, G., Nishimura, M., Arawaka, S., Levitan, D., Zhang, L., Tandon, A., Song, Y. Q., Rogaeva, E., Chen, F., Kawarai, T., Supala, A., Levesque, L., Yu, H., Yang, D. S., Holmes, E., Milman, P., Liang, Y., Zhang, D. M., Xu, D. H., Sato, C., Rogaeva, E., Smith, M., Janus, C., Zhang, Y., Aebersold, R., Farrer, L. S., Sorbi, S., Bruni, A., Fraser, P., and St. George-Hyslop, P. (2000) Nicastrin modulates presenilin-mediated notch/glp-1 signal transduction and  $\beta$ APP processing, *Nature* 407, 48–54.
- Francis, R., McGrath, G., Zhang, J., Ruddy, D. A., Sym, M., Apfeld, J., Nicoll, M., Maxwell, M., Hai, B., Ellis, M. C., Parks, A. L., Xu, W., Li, J., Gurney, M., Myers, R. L., Himes, C. S., Hiesch, R., Ruble, C., Nye, J. S., and Curtis, D. (2002) Aph-1 and pen-2 are required for Notch pathway signaling,  $\gamma$ -secretase cleavage of  $\beta$ APP, and presenilin protein accumulation, *Dev. Cell* 3, 85–97.
- Wolfe, M. S., Xia, W., Ostaszewski, B. L., Diehl, T. S., Kimberly, W. T., and Selkoe, D. J. (1999) Two transmembrane aspartates in presenilin-1 required for presenilin endoproteolysis and  $\gamma$ -secretase activity, *Nature* 398, 513–517.
- Li, Y., Xu, M., Lai, M., Huang, Q., Castro, J., DiMuzio-Mower, J., Harrison, T., Lellis, C., Nadin, A., Neduvilil, J., Register, R., Sardana, M., Shearman, M., Smith, A., Shi, X., Yin, K., Shafer, J., and Gardell, S. (2000) Photoactivated  $\gamma$ -secretase inhibitors directed to the active site covalently label presenilin 1, *Nature* 405, 689–694.
- Esler, W., Kimberly, W., Ostaszewski, B., Diehl, T., Moore, C., Tsai, J., Rahmati, T., Xia, W., Selkoe, D., and Wolfe, M. (2000) Transition-state analogue inhibitors of  $\gamma$ -secretase bind directly to presenilin-1, *Nat. Cell Biol.* 2, 428–434.
- Seiffer, D., Bradley, J., Rominger, C., Rominger, D., Yang, F., Meredith, J., Jr., Wang, Q., Roach, A., Thompson, L., Spitz, S., Higaki, J., Prakash, S., Combs, A., Copeland, R., Arneric, S., Haitig, P., Robertson, D., Cordell, B., Stern, A., Olson, R., and Zaczek, R. (2000) Presenilin-1 and -2 are molecular targets for  $\gamma$ -secretase inhibitors, *J. Biol. Chem.* 275, 34086–34091.
- Herreman, A., Hartmann, D., Annaert, W., Saftig, P., Craessaerts, K., Serneels, L., Umans, L., Schrijvers, V., Checler, F., Vanderstichele, H., Baekelandt, V., Dressel, R., Cupers, P., Huylebroeck, D., Zwijsen, A., Van Leuven, F., and De Strooper, B. (1999) Presenilin 2 deficiency causes a mild pulmonary phenotype and no changes in amyloid precursor protein processing but enhances the embryonic lethal phenotype of presenilin 1 deficiency, *Proc. Natl. Acad. Sci. U.S.A.* 96, 11872–11877.
- Saura, C. A., Choi, S. Y., Beglopoulos, V., Malkani, S., Zhang, D. M., Shankaranarayana Rao, B. S., Chattarji, S., Kelleher, R. J. R., Kandel, E. R., Duff, K., Kirkwood, A., and Shen, J. (2004) Loss of presenilin function causes impairments of memory and synaptic plasticity followed by age-dependent neurodegeneration, *Neuron* 42, 23–36.
- Qyang, Y., Chambers, S. M., Wang, P., Xia, X., Chen, X., Goodell, M. A., and Zheng, H. (2004) Myeloproliferative disease in mice with reduced presenilin gene dosage: Effect of  $\gamma$ -secretase blockage, *Biochemistry* 43, 5352–5359.
- Edbauer, D., Winkler, E., Regula, J. T., Pesold, B., Steiner, H., and Haass, C. (2003) Reconstitution of  $\gamma$ -secretase activity, *Nat. Cell Biol.* 5, 486–488.
- Goutte, C., Tsunozaki, M., Hale, V. A., and Priess, J. R. (2002) APH-1 is a multipass membrane protein essential for the Notch signaling pathway in *Caenorhabditis elegans* embryos, *Proc. Natl. Acad. Sci. U.S.A.* 99, 775–779.
- Guo, Q., Sebastian, L., Sopher, B. L., Miller, M. W., Ware, C. B., Martin, G. M., and Mattson, M. P. (1999) Increased vulnerability of hippocampal neurons from presenilin-1 mutant knock-in mice to amyloid  $\beta$ -peptide toxicity: Central roles of superoxide production and caspase activation, *J. Neurochem.* 72, 1019–1029.
- Levitan, D., Lee, J., Song, L., Manning, R., Wong, G., Parker, E., and Zhang, L. (2001) PS1 N- and C-terminal fragments form a complex that functions in APP processing and Notch signaling, *Proc. Natl. Acad. Sci. U.S.A.* 98, 12186–12190.
- Zhang, L., Song, L., Terracina, G., Liu, Y., Pramanik, B., and Parker, E. (2001) Biochemical characterization of the  $\gamma$ -secretase activity that produces  $\beta$ -amyloid peptides, *Biochemistry* 40, 5049–5055.
- Li, Y., Lai, M., Xu, M., Huang, Q., DiMuzio-Mower, J., Sardana, M., Shi, X., Yin, K., Shafer, J., and Gardell, S. (2000) Presenilin 1 is linked with  $\gamma$ -secretase activity in the detergent solubilized state, *Proc. Natl. Acad. Sci. U.S.A.* 97, 6138–6143.
- Boulianne, G. L., Livne-Bar, I., Humphreys, J. M., Liang, Y., Lin, C., Rogaeva, E., and P., S. G.-H. (1997) Cloning and characterization of the Drosophila presenilin homologue, *NeuroReport* 8, 1025–1029.
- Zhang, L., Song, L., and Parker, E. (1999) Calpain inhibitor I increases  $\beta$ -amyloid peptide production by inhibiting the degradation of the substrate of  $\gamma$ -secretase, *J. Biol. Chem.* 274, 8966–8972.
- Borchelt, D. R., Thinakaran, G., Eckman, C. B., Lee, M. K., Davenport, F., Ratovitsky, T., Prada, C. M., Kim, G., Seekins, S., Yager, D., Slunt, H. H., Wang, R., Seeger, M., Levey, A. I., Gandy, S. E., Copeland, N. G., Jenkins, N. A., Price, D. L., Younkin, S. G., and Sisodia, S. S. (1996) Familial Alzheimer's

- disease-linked presenilin 1 variants elevate  $A\beta_{1-42/1-40}$  ratio in vitro and in vivo, *Neuron* 17, 1005–1013.
28. Ancolio, K., Dumanchin, C., Barelli, H., Warter, J. M., Brice, A., Campion, D., Frebourg, T., and Checler, F. (1999) Unusual phenotypic alteration of  $\beta$ -amyloid precursor protein ( $\beta$ APP) maturation by a new Val-715  $\rightarrow$  Met  $\beta$ APP-770 mutation responsible for probable early-onset Alzheimer's disease, *Proc. Natl. Acad. Sci. U.S.A.* 96, 4119–4124.
  29. Chen, F., Gu, Y., Hasegawa, H., Ruan, X., Arawaka, S., Fraser, P., Westaway, D., Mount, H. T., and St. George-Hyslop, P. (2002) Presenilin 1 mutations activate  $\gamma$  42-secretase but reciprocally inhibit  $\epsilon$ -secretase cleavage of amyloid precursor protein (APP) and S3-cleavage of notch, *J. Biol. Chem.* 277, 36521–36526.
  30. Murphy, M. P., Uljon, S. N., Golde, T. E., and Wang, R. (2002) FAD-linked mutations in presenilin 1 alter the length of  $A\beta$  peptides derived from  $\beta$ APP transmembrane domain mutants, *Biochim. Biophys. Acta* 1586, 199–209.
  31. Levitan, D., Doyle, T. G., Brousseau, D., Lee, M. K., Thinakaran, G., Slunt, H. H., Sisodia, S. S., and Greenwald, I. (1996) Assessment of normal and mutant human presenilin function in *Caenorhabditis elegans*, *Proc. Natl. Acad. Sci. U.S.A.* 93, 14940–14944.
  32. O'Reilly, D. R., Miller, L. K., and Luckow, V. A. (1994) *Baculovirus expression vectors: A laboratory manual*, Oxford University Press, New York.
  33. Gu, Y., Chen, F., Sanjo, N., Kawarai, T., Hasegawa, H., Duthie, M., Li, W., Ruan, X., Luthra, A., Mount, H. T., Tandon, A., Fraser, P. E., and St. George-Hyslop, P. (2003) APH-1 interacts with mature and immature forms of presenilins and nicastrin and may play a role in maturation of presenilin-nicastrin complexes, *J. Biol. Chem.* 278, 7374–7380.
  34. Takasugi, N., Tomita, T., Hayashi, I., Tsuruoka, M., Niimura, M., Takahashi, Y., Thinakaran, G., and Iwatsubo, T. (2003) The role of presenilin cofactors in the  $\gamma$ -secretase complex, *Nature* 422, 438–441.
  35. Kimberly, W. T., LaVoie, M. J., Ostaszewski, B. L., Ye, W., Wolfe, M. S., and Selkoe, D. J. (2003)  $\gamma$ -Secretase is a membrane protein complex comprised of presenilin, nicastrin, Aph-1, and Pen-2, *Proc. Natl. Acad. Sci. U.S.A.* 100, 6382–6387.
  36. Hayashi, I., Urano, Y., Fukuda, R., Isoo, N., Kodama, T., Hamakubo, T., Tomita, T., and Iwatsubo, T. (2004) Selective reconstitution and recovery of functional  $\gamma$ -secretase complex on budded baculovirus particles, *J. Biol. Chem.* 279, 38040–38046.

BI0481500